Environmental Impact Assessment Review 117 (2026) 108235

Contents lists available at ScienceDirect

Environmental Impact Assessment Review

journal homepage: www.elsevier.com/locate/eiar

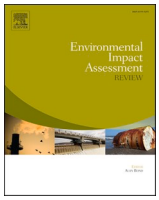

Toward a more reliable evaluation of CO_2 emissions from the firing stage of ceramic tiles within the life cycle assessment (LCA) methodology

Andrei Ungureanu [a,b,*], Antonella Sola [a,b], Paolo Neri [a], Roberto Rosa [a,b], Alessandro Gualtieri [c], Anna Maria Ferrari [a,b]

[a] Department of Sciences and Methods for Engineering, University of Modena and Reggio Emilia, via Amendola 2, 42122 Reggio Emilia, Italy
[b] Interdepartmental Center En&Tech, University of Modena and Reggio Emilia, Tecnopolo di Reggio Emilia, Piazzale Europa 1, 42123 Reggio Emilia, Italy
[c] Department of Chemical and Geological Sciences, University of Modena and Reggio Emilia, via Giuseppe Campi, 103, 41125 Modena, Italy

ARTICLE INFO

Keywords:
Life cycle assessment
Ceramic industry
Organic carbon
Structural water loss
Clays
Carbon footprint
Climate change

ABSTRACT

The need for a more realistic evaluation of the environmental impacts caused by hard-to-abate industrial sectors, such as ceramic tiles production, is essential in order to meet the European Union (EU) target for carbon neutrality by 2050. This implies that the environmental impact assessment of ceramic processes must also account for the emissions of CO_2 arising from sources different from the natural gas combustion upon firing, with the latter being typically the only CO_2 considered according to the stoichiometry of the combustion reaction. The current study proposes a method for determining the CO_2 emissions associated with the physicochemical transformations occurring while firing the ceramic body. By integrating chemical and mineralogical composition, structural water loss estimation, and loss on ignition data, this approach enables the inclusion of these emissions in the Life Cycle Inventory (LCI) phase of Life Cycle Assessment (LCA). A comparative LCA, based on a reference flow of 1 m^2 of porcelain stoneware tile, average thickness of 9.5 mm, corresponding to a mass of 24.5 kg, showed that including these additional emissions results in an 8.4 % increase in climate change compared to conventional assessments that only consider CO_2 from natural gas combustion. Furthermore, the study challenges the conventional climate-neutrality assumption applied to biogenic CO_2 by assigning a Global Warming Potential (GWP) of 1 to emissions from organic matter in clay minerals—an application not previously addressed in LCA literature. This novel framework not only enhances the accuracy of carbon accounting in ceramic tile manufacturing but also provides a versatile methodology that can be applied across various ceramic products. By addressing previously overlooked emission sources, the study contributes to more realistic environmental impact assessments, supporting the EU's carbon neutrality goals and informing policy, industry practices, and future LCA standards.

1. Introduction

Technological evolution and increased responsiveness to market requirements have significantly enhanced existing ceramic products and manufacturing processes, while also fostering the creation of novel ceramic styles. However, it is essential to acknowledge that ceramic manufacturing processes remain energy-intensive and environmentally impactful, particularly due to their reliance on fossil fuels, namely natural gas. It has been estimated that, within the European Union, ceramic manufacturing processes (including bricks, floor and wall tiles, and refractories) contribute to an annual emission of 19 Mt. of CO_2 (Furszyfer Del Rio et al., 2022). In ceramic tile manufacturing processes, for instance, three production phases – namely, spray drying, drying, and firing – are responsible for a high level of non-renewable fossil fuel consumption, raising concerns about this sector's environmental consequences.

The development of effective industrial pollutant control strategies is a key area of research, with studies investigating advanced methods for treating both liquid and gaseous effluents. For instance, recent work in wastewater treatment has demonstrated how optimising sludge properties can significantly mitigate membrane fouling and improve pollutant removal (Zhang et al., 2021). These insights underscore the

* Corresponding author at: Department of Sciences and Methods for Engineering, University of Modena and Reggio Emilia, via Amendola 2, 42122 Reggio Emilia, Italy.
E-mail address: andrei.ungureanu@unimore.it (A. Ungureanu).

https://doi.org/10.1016/j.eiar.2025.108235
Received 26 June 2025; Received in revised form 3 October 2025; Accepted 16 October 2025
Available online 24 October 2025

importance of integrating pollutant control innovations into the industry, particularly in sectors that are responsible for significant amounts of emissions, such as ceramic sector.

Unlike other substances, CO_2 emissions in industrial settings are not directly measured (Kates et al., 1998), instead, they are calculated as the theoretical amount released from the combustion of fossil fuels in power plants. The estimation of greenhouse gas (GHG) emissions from industrial processes relies on the average calorific data for the corresponding fossil fuel (Keeling, 1973). However, in industry, there are other sources of CO_2 emissions such as the decomposition of inorganic carbonates and the combustion of organic matter upon thermal treatment of raw materials.

Currently, the predominant methodology employed to quantify the potential environmental impacts, including—but not limited to—climate change caused by GHG emissions is Life Cycle Assessment (LCA). LCA serves as a reliable tool for determining the environmental impacts associated with products and processes. It is defined as "the compilation and evaluation of the inputs, outputs, and potential environmental impacts of a product system throughout its life cycle" (ISO 14040, 2006). The LCA process encompasses four key steps: (i) goal and scope definition, which involves articulating the purpose of the study, defining the functional unit, scoping the product system, setting the system's boundaries, the geographical and temporal boundaries, and deciding the modelling approach (attributional or consequential); (ii) life cycle inventory (LCI), which entails the detailed accounting of the inputs (materials, energy, resources) and outputs of the system (products, waste treatment, atmospheric emissions); (iii) life cycle impact assessment (LCIA), where the inputs and outputs are categorized into impact categories and quantified into potential environmental impacts; (iv) interpretation, which involves a critical analysis of the results in the context of the study's goals (Hellweg et al., 2014).

Recent reviews on LCA of ceramic tiles (Vieira et al., 2023) have identified the firing step as the most impactful phase leading to substantial GHG emissions. Accordingly, climate change emerges as the most discussed impact factor in the majority of the performed studies. Particularly, porcelain stoneware, the top tile product in the marketplace, requires extremely high firing temperatures of 1200–1250 °C, leading to a huge consumption of natural gas, and therefore, massive emissions of CO_2 and other airborne pollutants such as nitrogen and sulfur oxides (Almeida et al., 2016).

LCA studies of ceramic tiles have traditionally focused on transports, packaging, energy consumption and fossil-derived emissions of CO_2. While fossil fuel combustion processes are certainly the main cause of GHG emissions, it is critical to note that the current LCA studies of ceramic tiles exclude from their output inventories the CO_2 emissions stemming from both organic matter combustion and inorganic carbonates decomposition tied to the raw materials being used, and this leads to a non-negligible underestimation of the climate change impact category. This omission is primarily attributed to the challenges associated with the inherent complexity of the physicochemical phenomena occurring upon firing, and to the difficulty of accurately quantifying the content of organic matter within the ceramic raw materials. Although some recent LCA studies of ceramic materials employed flue gas analyser techniques (Rauf et al., 2022), the current European legislation does not mandate their use, instead favouring standardized calculation methods for consistency, cost-effectiveness, and operational feasibility.

The firing process of ceramic tiles is notably intricate owing to a multitude of concurrent physicochemical transformations. Some of the reported processes are the dehydration and dehydroxylation of clays, the combustion of organic matter, the α-quartz to β-quartz phase transition, the decomposition of carbonates (e.g., calcite and dolomite), the sintering processes that may include liquid phase formation, crystallization and densification, the glassy phase formation promoted by the melting of feldspars and many more (Ferrer et al., 2015; Djemli et al., 2023).

The mass reduction of a ceramic tile upon firing is defined as the loss on ignition (LOI). In the field of soil science, LOI typically measures the amount of organic matter that is present in a mineral soil. However, studies have demonstrated that this method, if applied to ceramic tiles, can result in significant inaccuracies, as it fails to account for the presence of inorganic carbonates or structural water within clay minerals. Hence, in order to reliably quantify the emissions of CO_2 associated with the thermal treatment of ceramic raw materials, it is imperative to determine the amounts of both organic matter and inorganic carbonates within the raw materials. Given the limitations of the LOI method, an alternative calculation method must be proposed.

This study aims to develop a robust and replicable protocol for determining the content of organic matter and inorganic carbonates in ceramic raw materials, grounded in their chemical and mineralogical composition. By quantifying the CO_2 emissions generated during the firing process—specifically those arising from the decomposition of inorganic carbonates and the combustion of organic matter—and incorporating them into the LCA framework, the study addresses a key limitation in current environmental evaluations, which often exclude materials-related emissions. The approach integrates chemical and mineralogical composition, structural water loss estimation, and loss on ignition data, to more accurately estimate the emissions caused by the production of ceramic tiles.

In addition, the study challenges the conventional climate-neutrality assumption applied to biogenic CO_2 by evaluating, for the first time, the GWP of the CO_2 associated with organic carbon stored within clay minerals. While GWP values have previously been assessed for biogenic CO_2 from sources such as wood biomass (Liu et al., 2017; Cherubini et al., 2012), no such evaluation has been conducted for the organic matter naturally present in mineral matrices.

The proposed methodology is adaptable to a variety of ceramic products, including bricks, refractories, and sanitaryware, and supports more informed decisions in raw material selection, more transparent environmental reporting, an effective shift toward lower-impact production practices within the sector.

2. Materials and methods

2.1. Formulation of the stoneware tile ceramic body

Natural raw materials have played a pivotal role in the evolution of ceramic production. Over the years, rigorous assessments have been conducted to understand their chemical composition, mineralogical properties, particle size distribution, and their effect on ceramic properties.

The three major natural raw materials that form the stoneware tile ceramic body are clays, feldspars and quartz-rich sands. A number of additional natural and synthetic raw materials can be added in various proportions to the ceramic mix to impart the desired properties to the finished product. Among them carbonates, talc, wollastonite, alumina, zircon. Deflocculating agents such as sodium silicate are also added in minor amounts (generally <0.3–0.5 wt%).

Clay minerals belong to the family of layer silicates, two-dimensional structures composed of sheets of Si- (and Al-) centred tetrahedra attached to Al- (gibbsite-like) or Mg-(brucite-like) centred octahedral sheets. When Al (III) occupies 2/3 of the octahedral cavities, a dioctahedral structure is formed whereas when Mg (II) occupies all (3/3) the octahedral cavities, a trioctahedral structure is formed (Arabmofrad et al., 2020). Fe (II) and/or Fe (III) is also generally found in the octahedral sheets. The three major clay minerals found in stoneware tile ceramic mixes are kaolinite, illite, and smectite.

Kaolinite (ideally $Al_2(OH)_4Si_2O_5$) is the most common clay mineral on Earth and by far the major clay raw material used in the production of ceramics. It is a 1:1 7 Å layer silicate composed of one Si-centred tetrahedral (T) sheet and one Al-dioctahedral (O) sheet. Hydroxyl groups responsible for the hydrogen bridging of T-O units are found in the so-called interlayer region (Brigatti et al., 2013). Illite is a

dioctahedral K-deficient mica with a 2:1 10 Å unit composed of two Si-centred tetrahedral (T) sheets and one sandwiched Al-centred dioctahedral (O) sheet (Brigatti et al., 2013; Gualtieri and Ferrari, 2006). The interlayer region hosts the compensating cation K and water molecules so that a mean ideal chemical formula is $K_{0.6}(H_3O^+)_{0.4}Al_2(OH)_2Si_{3.4}Al_{0.6}O_{10}$. Mg and Fe can replace Al in the octahedral layer. Smectite actually refers to a family of complex layer silicates whose montmorillonite is the major species. It is a dioctahedral phase with a 2:1 14 Å unit composed of two Si/Al-centred tetrahedral (T) sheets and one sandwiched Al-centred dioctahedral (O) sheet. Compensating cations (Ca^{2+}, K^+, Na^+) coordinated by water molecules are hosted in the interlayer region. An ideal formula of Ca-montmorillonite is $Ca_{x+y}(Al_{2-y}Mg_y)(OH)_2(Si_{4-x}Al_x)O_{10}\cdot nH_2O$ (Viani et al., 2025). Smectite species display different chemistry, structures (see below) and hence, different properties (Akisanmi, 2022). Minor amounts of the iron-rich chlorite clay minerals can also be present in natural clay raw materials. Chlorite is a non-swelling clay with a 2:1:1 unit showing negatively charged TOT sheets, alternating with positively charged brucite like ($Mg(OH)_2$) octahedral sheets (Tate, 2005; *Soil and Environmental Chemistry*, 2017). Chlorite is actually a term indicating a family of di-trioctahedral layer silicates with clinochlore ($Mg_5Al(OH)_8Si_3AlO_{10}$) and chamosite ($Fe_5Al(OH)_8Si_3AlO_{10}$) as end-member species (Brindley and Gillery, 2025).

Feldspars are anhydrous framework aluminosilicates of potassium ($KAlSi_3O_8$), sodium ($NaAlSi_3O_8$) and calcium ($CaAl_2Si_2O_8$), used in the ceramic body to promote sintering and vitrification (*gresification*). Sodium and calcium feldspars form a solid solution (plagioclase series), with albite ($NaAlSi_3O_8$) and anorthite ($CaAl_2Si_2O_8$) as low-temperature and high-temperature melting end-members, respectively.

The third major component of the stoneware tile ceramic mix is the quartz-rich sand which is added as inert backbone of the ceramic body (Gualtieri, 2007).

In the present study, a stoneware tile ceramic body composition was selected to exemplify the typical production practices of a prominent company located in the Sassuolo district, the epicentre of Italian ceramic manufacturing. This composition is representative of the Italian ceramic tile industry and comprises 41.0 % clays, 44.5 % feldspars, 12.6 % quartz-rich sands, along with minor constituents such as alumina (1 %) and sodium silicate (<1 %) employed as a deflocculating agent. Flint pebbles serve as the grinding media during the milling phase of ceramic production. A negligible quantity of these pebbles (<0.1 %) remains embedded within the ceramic body, as determined by weight loss measurements, and this variance was accounted for in the study. The chemical and mineralogical composition of the raw materials used in this study for the ceramic body mix was retrieved from the literature, as detailed in Table 1.

The selected representative composition of the ceramic body contains five types of clays (i.e., Cl1-Cl5), with different chemical, mineralogical and physical characteristics (Table 1). For instance, the Ukrainian clay (i.e., Cl1) consists of fine kaolinite-rich particles and contains low amounts of quartz, exhibiting unique technological properties such as high plasticity, viscosity, low compressibility, and fast sintering kinetics (Zanelli et al., 2015). High iron-containing clays (i.e., Cl4 and Cl5) are used in small amounts, mainly due to the fact that they degrade the technological and aesthetical properties of the ceramic tile (Andji et al., 2009). Small amounts of high plasticity clays (i.e., bentonite, "BE") are used in order to improve the mechanical strength (Zaidan and Abdull-Razzak, 2018).

The formulation is rich in sodium feldspar (like Fd1 in Table 1) which significantly contributes to improving the properties of the ceramic tile, namely high bulk density, low percent water adsorption and high flexural strength (Das and Dana, 2003).

Quartz is found in both the clay and feldspars components.

2.2. Loss on ignition

The Loss on ignition (LOI) method involves determining the mass reduction of the ceramic body upon firing. It is commonly used to estimate the amount of organic carbon contained in the raw materials (Ball, 1964). However, the reliability of this method is often questionable, particularly for materials rich in clays. Two factors that contribute to the lack of accuracy of LOI method are:

1. Release of CO_2 from carbonates. During firing, carbonates such as calcite, magnesite or dolomite decompose, releasing CO_2. This weight loss can be mistakenly attributed to organic carbon (Heiri et al., 2001).
2. Release of structural water. Silicate minerals contain water molecules physically and chemically bound within their crystal structure (Hoogsteen et al., 2015). As the ceramic body heats up, this water is

Table 1
The average weight percentage content, chemical composition of raw materials for ceramic body and mineralogical composition for clay minerals. Abbreviations: Cl = clay; BE = bentonite, a natural raw material with >50 wt% of smectite; Fd = feldspar Cl = clay; kao = kaolinite; ill = illite; smc = smectite; chl = chlorite; ms = muscovite; qz = quartz; Fe-ox = iron oxy-hydroxydes; cal = calcite.

Mineral	Origin	wt%	SiO_2	Al_2O_3	TiO_2	Fe_2O_3	MgO	CaO	Na_2O	K_2O	LOI
Cl1 (Zanelli et al., 2015)	Ukraine	30.0	59.70	26.00	1.20	1.00	0.70	0.40	0.40	2.10	8.20
Cl2 (Celik, 2010)	Turkey	4.60	55.85	26.46	1.20	3.23	0.58	0.34	0.11	2.00	10.00
Cl3 (Galos, 2011)	Germany	3.80	70.90	18.10	1.16	0.85	0.22	0.12	0.20	2.06	7.03
Cl4 (Dondi et al., 1999)	Italy	1.20	64.60	15.80	0.80	6.20	2.10	2.30	0.90	1.80	7.10
Cl5 (Dondi and Fabbri, 1993)	Italy	1.30	57.20	15.50	0.70	6.00	2.70	5.20	1.00	1.80	8.90
BE (Karnland, 2025)	Turkey	0.10	65.90	21.50	0.24	4.46	0.40	5.20	2.70	0.60	9.20
Fd1 (Di Primio, 2018)	Turkey	22.00	72.00	17.00	0.32	0.15	0.06	0.40	9.80	0.40	0.40
Fd2 (Di Primio, 2018)	Italy	0.08	77.00	12.50	0.09	1.00	0.10	0.10	0.50	7.30	1.70
Fd3 (Palomba et al., 2010)	Italy	8.20	68.93	16.65	0.37	2.78	0.58	0.29	1.57	7.11	1.50
Fd4 (Minerali Industriali S.r.l, 2016)	Italy	12.60	87.00	6.00	0.05	0.05	0.05	0.10	0.20	5.00	0.50
Fd5 (Odent, 1994)	France	14.20	70.70	17.20	0.17	0.36	0.20	0.65	4.40	4.30	2.20
Alumina	France	1.00	–	100.00	–	–	–	–	–	–	–
Sodium silicate	Italy	0.80	16.50	83.50	–	–	–	–	–	–	–
Flint pebbles	Italy	0.10	100.00	–	–	–	–	–	–	–	–
	Average mineralogical composition of clay minerals										
		kao	ill	smc	chl	ms	qz	Fe-ox	cal		fd
Cl1 (Zanelli et al., 2015)		44.00	31.00	–	–	–	21.00	1.00	1.00		2
Cl2 (Celik, 2010)		49.00	20.00	1.30	–	–	29.00	0.00	0.57		–
Cl3 (Galos, 2011)		32.00	5.00	1.00	–	–	61.20	0.69	0.18		–
Cl4 (Dondi et al., 1999)		10.60	21.20	8.55	7.95	–	47.50	0.40	3.80		–
Cl5 (Dondi and Fabbri, 1993)		5.00	30.30	7.00	9.50	–	39.00	0.0	9.11		–
BE (Karnland, 2025)		–	0.80	82.50	–	3.50	2.6	4.4	0.67		4.6

released over a wide range of temperatures, severely affecting weight measurements.

For ceramic materials, the LOI is experimentally determined by heating a sample that has been pre-dried overnight at 105–110 °C to a temperature range of 900–1100 °C (Rat et al., 2023). Humidity water is lost up to 105–110 °C but the ceramic body may still retain water which is released at higher temperature. Clay minerals contain zeolitic and structural water. Zeolitic water refers to water molecules or hydronium ions hosted in the interlayer volume of illite and smectite and is typically removed by heating to relatively moderate temperatures (100–250 °C). Structural water refers to the hydroxyl groups which are part of the crystal lattice of hydrates silicates (layer silicates and amphiboles). They are released through a dehydroxylation reaction over a wide temperature range (400–1050 °C) (Taylor, 1962).

As for clay minerals, the LOI values are influenced by several factors, including the crystal structure, chemistry, presence of impurities, and the temperature at which the experiment is performed. For instance, most experiments documented in the literature were conducted below 550 °C, under the decomposition temperature of inorganic carbonates (Table S1 of Supporting Information, SI). The precision of the results depends on the number of analysed samples. Moreover, as anticipated above, the loss of structural water occurs over a wide temperature range, depending on the mineralogical structure, introducing a potential source of errors. For example, the dehydroxylation of smectites occurs in between 300 and 900 °C (Derkowski and Kuligiewicz, 2022), whereas the dehydroxylation of illite occurs at temperatures between 550 and 900 °C (Gualtieri and Ferrari, 2006; Wang et al., 2017).

In order to account for these factors contributing to the weight loss upon firing, more precisely, the LOI is defined as the sum of three components (Eq. (1)): the total zeolitic and structural water loss (SWL), the amount of CO_2 released from inorganic carbonates (IC), and the quantity of organic matter (OM).

$$LOI = SWL + IC + OM \tag{1}$$

The determination of the content of organic carbon (OC) within the organic matter (OM) can be achieved experimentally in various ways such as Tinsley method, Walkley Black (WB) method, C analyser and dry combustion. However, noticeable differences have been observed between these methods, and this introduces potential sources of errors in choosing one method over the other (Ramamoorthi and Meena, 2018).

A literature review of the linear regression equations describing the dependence of LOI on OC is presented in Table S1. Although a number of equations have been developed throughout the years, there is no general equation that allows for an objective estimation of the OC content of minerals, since most of the well-known linear regressions have been determined based on experimental data pertaining to specific geographic areas, climate conditions and soil nature. The difficulty in applying any of these equations in a general study for correlating LOI and OC is mostly due to the SWL, as well as to the fact that the OC content is strongly dependent on the soil mineralogy and chemical composition.

Other sources of volatiles that affect the LOI and OC correlation include sulfates like gypsum ($CaSO_4{\cdot}2H_2O$), which release zeolitic water + SO_3; amphiboles like tremolite ($Ca_2Mg_5Si_8O_{22}(OH)_2$), which release hydroxyl groups and are present as impurities in many natural raw materials; dolomite ($CaMg(CO_3)_2$), which releases CO_2; talc ($Mg_3(OH)_2Si_4O_{10}$) and halloysite ($Al_2(OH)_2Si_4O_{10}{\cdot}2H_2O$), which release hydroxyl groups. These minerals are not considered in the present contribution, because they are not typically found in the body mixes for the formulation of stoneware ceramic tiles in Europe, but can be found in other regions in the world. However, small amounts of limonite/goethite FeO(OH), releasing hydroxyl groups upon heating, were included in the calculations for this study.

2.3. Calculation of SWL for the clay minerals in the formulation of the ceramic body

SWL is the main source of error for the determination of the OM, and hence, the OC content, within clay minerals when employing the LOI method. A theoretical quantification of the structurally bound water is essential to provide a good estimation of the total content of OC in the ceramic body.

To estimate the SWL of the ceramic body, Eq. (2) can be utilized, where SWL_i is the individual SWL for each distinct clay type constituting the ceramic body and X_i denotes the corresponding mass fraction (Sun et al., 2009).

$$SWL = \sum_{i=1}^{n} SWL_i{\cdot}X_i \tag{2}$$

As already reported above, here the term "structural water" of minerals comprises two distinct components, namely the zeolitic hydration water molecules (H_2O) and the hydroxyl groups (OH^-) (Sun et al., 2009). The release of structural water upon heating involves complex reaction mechanisms, where initially, the hydration water is lost, followed by the dehydroxylation that requires a higher energy input. Kinetic studies and molecular simulations have been leveraged for the determination of the mechanisms of dehydroxylation; however, the total quantification of structural water is yet to be perfectioned.

When it comes to ceramic raw materials, for the effective measurement of the LOI, a major part of the hydration water is lost during predrying. However, thermogravimetric analyses have shown that for expanding clays such as smectites, some part of the hydration water may persist until 200–250 °C[45], which indicates that the reported LOI for clay minerals with high content of smectites contains in fact some amount of dehydration water, denoted as "H_2O-", as well as the dehydroxylation water, denoted as "H_2O+".

The results obtained in this study for the average SWL of each clay mineral are summarized in Table 2.

As far as kaolinite is concerned, the dehydroxylation reaction is well described in the literature (Gasparini et al., 2013). Although we are aware that recently Cheng et al. (Cheng et al., 2019) identified three types of hydroxyl groups in kaolinite, and estimated that 10 % of these hydroxyl groups cannot be removed by flash calcination at 1300 °C, here we consider the stoichiometric dehydroxylation reaction, leading to the formation of metakaolinite and water vapour: $Al_2(OH)_4Si_2O_5 \rightarrow Al_2Si_2O_7 + 2H_2O$ ($n_{H_2O} = 2.0$, see Table 2).

The dehydroxylation of illite occurs in a multistep sequence, with at least one low-temperature step and one high-temperature step. This sequence includes the condensation of water molecules in the octahedral layer, the one-dimensional diffusion of the water molecules through the tetrahedral rings of the silica layer, and the two-dimensional diffusion of the water molecules across the interlayer region, which is considered the rate limiting step (Gualtieri and Ferrari, 2006). The thermal transformation of illite firstly involves the conversion into dehydroxylated muscovite, followed by the breakdown into mullite crystals, above 1100 °C[42]. Here, we considered the ideal formula for illite (i.e., $K_{0.6}(H_3O)_{0.4}Al_{2.0}(OH)_2Si_{3.4}Al_{0.6}O_{10}$), leading to $n_{H_2O} = 1.0$, as indicated in Table 2.

Although the mechanisms of montmorillonite dehydroxylation are not completely understood, it has been postulated that dehydroxylation starts at the mineral surface, and it proceeds through the formation of several intermediate, irreversible phases, leading to an unstable mixture of five and six coordinated octahedral forms (Drits et al., 1995; Stevenson and Gurnick, 2016). Experimental studies have shown that for Ca-montmorillonite, dehydration occurs up to 240 °C, whereas dehydroxylation occurs at approximately 720 °C (Ogloza and Malhotra, 1989). Beyond 1000 °C, most montmorillonites transition to spinel structure (Stevenson and Gurnick, 2016). Other experimental studies have indicated that the dehydration of smectites can be achieved by

Table 2
The calculated average structural water loss (SWL) for the clay minerals that constitute the ceramic body.

Layer silicate	Chemical Formula	Dehydroxylation Product	n_{H_2O}	SWL wt%
illite	$K_{0.6}(H_3O)_{0.4}Al_{2.0}(OH)_2Si_{3.4}Al_{0.6}O_{10}$	$K_{0.6}Al_{2.6}Si_{3.4}O_{11}$	1	4.60
kaolinite	$Al_2(OH)_4Si_2O_5$	$Al_2Si_2O_7$	2	13.95
mont-morillonite	$Ca_{0.2}Al_2(OH)_2Si_4O_{10}(H_2O)_{0.7}$	$Ca_{0.2}Al_2Si_4O_{11}$	1.7	8.30
chlorite (clinochlore)	$(Mg_2Al)Mg_3(OH)_8(Si_3Al)O_{10}$	$Mg_5Al_2Si_3O_{14}$	4	11.65
muscovite	$KAl_2(OH)_2(Si_3Al)O_{10}$	$KAl_3Si_3O_{11}$	1	4.52

heating the sample at 300 °C overnight, without involving dehydroxylation, yielding an (experimentally measured) average of 3.17 wt% hydration water in between 110 °C and 300 °C[45]. This value is notably lower than the experimental results obtained by Garg et al. (Garg and Skibsted, 2014) for pure montmorillonite, which showed 4.58 % SWL in the range 110–550 °C, mostly attributed to the initiation of dehydroxylation above 300 °C. In the present study, the montmorillonite hydration water content above 110 °C was approximated according to the findings of Cuadros et al. (Cuadros et al., 1994), and the hydration water loss was calculated according to the equation: $Ca_{0.2}Al_2(OH)_2Si_4O_{10}(H_2O)_{0.7} \rightarrow Ca_{0.2}Al_2Si_4O_{11} + 1.7H_2O$, resulting in a hydration water loss number , $n_{H_2O} = 1.7$ (See Table 2).

As far as chlorite is concerned, the theoretical content of water for chlorites as OH^- groups is approximately 13.0 wt% ($n_{H_2O} = 4$), and the dehydroxylation temperature depends on the content of Mg, with a maximum of 860 °C (Zhan and Guggenheim, 1995; Steudel et al., 2016).

Although it is not actually a clay mineral, the layer silicate mica muscovite is often accompanied to illite. Muscovite is also a dioctahedral layer silicate with a 2:1 10 Å unit composed of two Si-centred tetrahedral (T) sheets and one sandwiched Al-centred dioctahedral (O) sheet. K is the compensating cation hosted in the interlayer region (Brigatti et al., 2013; Gualtieri and Ferrari, 2006). The dehydroxylation of muscovite occurs over a relatively wide temperature range of 800–1100 °C and the SWL is approximately 4.6 %, consistent with its empirical formula (Gridi-Bennadji et al., 2008), with $n_{H_2O} = 1$.

The computed SWL values obtained in this study for C11-C15 and for BE are presented in Table 3. The results indicate that the mineral samples whose clay content exceeds 70 % exhibit significantly elevated SWL values (i.e., Cl1 and Cl2). In contrast, samples with a clay content below 50 % (compensated by a higher proportion of quartz) experience a much lower SWL, falling below 5 % (i.e., Cl3, Cl4 and Cl5). These results emphasize the critical role of the nature and the relative amount of clay minerals in determining the amount of SWL experienced upon heating by the ceramic body.

2.4. LOI of feldspars

In the case of feldspars, they are anhydrous minerals and thus, their LOI is exclusively associated with the thermal decomposition of impurities like calcite and dolomite, and with the combustion of organic matter, due to the absence of structurally bound water. Here, the LOI values are solely attributed to the content of carbonates and organic matter as the feldspars used in this study have a low content of IC (<0.31 %), with OM contents ranging from 0.087 to 1.68 %, as detailed in Table S2. Other sources of volatiles, such as the hydroxyls present in amphibole impurities observed in some feldspar natural raw materials (e.g. tremolite, $Ca_2Mg_5Si_8O_{22}(OH)_2$, in albite feldspar from Sardinia (Gualtieri et al., 2018)) have not been considered here due to their rarity.

Table 3
The calculated average structural water loss (SWL), inorganic carbon (IC) and organic matter (OM) for the clay minerals that form the ceramic body.

Clay Mineral	SWL (%)	IC (%)	OM (%)
Cl1	7.66	0.44	0.095
Cl2	7.86	0.25	1.88
Cl3	4.84	0.082	2.10
Cl4	4.12	1.705	1.26
Cl5	3.77	4.00	1.18
BE	6.98	0.29	1.91

2.5. OM quantification

The amount of OM in the ceramic body can be estimated by deducing the sum of the calculated values for SWL and IC from the experimental values for the LOI (Eq. (1)). The amount of IC is calculated from the stoichiometry of the reaction of the decomposition of calcite. The results indicate that, on average, the ceramic body under examination (Table 1) contains a total of 0.64 wt% of OM. To evaluate the content of organic carbon (OC) within the OM, it was assumed that the OM comprises 80 % humic substances, and 10 % lignin, with the remaining being a combination of lipids, proteins, polysaccharides and cellulose in equal parts (Table S3) (Wang et al., 2023). This composition leads to an average of 51.7 % OC in the OM (Eq. (3), which aligns with the results previously reported for clay-rich soils (Jensen et al., 2018). Although slightly lower than the widely used van Bemmelen factor of 0.58 (Heaton et al., 2016), it reflects the generally lower OC content characteristic of clay-rich soils, making the assumption reasonable.

$$OC = 0.517 \cdot OM \tag{3}$$

The results obtained for the ceramic body composition considered in this study (Table 1) are summarized in Table 4. It is observed that there is a noticeable underestimation of the ceramic tile carbon emissions by 0.41 kg CO_2/m^2 (see last two columns), when the emissions associated with the chemical processes occurring within the ceramic body are disregarded.

2.6. Life cycle assessment

The Life Cycle Assessment (LCA) was conducted in accordance with the ISO 14040 and 14,044:2006 guidelines (ISO 14040, 2006; ISO 14044, 2006).

2.6.1. Goal and scope definition

The primary objective of this study is to quantify the potential environmental impacts associated with the firing process necessary for the production of 1 m^2 of ceramic tiles. The functional unit of the system is defined as 24.5 kg of fired ceramic material necessary for the

Table 4
Summary of the results for the assessment of the LOI of the ceramic body examined in this study. The amounts of IC and OC emitted are expressed in kg CO_2 per m^2 of finished ceramic tile product.

LOI (%)	SWL (%)	IC (%)	OM (%)	kg CO_2/m^2 (from IC)*	kg CO_2/m^2 (from OC)**
3.97	2.94	0.39	0.64	0.10	0.31

* Calculated as the stoichiometric amounts of CO_2 released from the decomposition of calcite and dolomite.

** Calculated as the stoichiometric amounts of CO_2 resulted from the combustion of organic matter (i.e., $OM = 0.517 \bullet MWCO_2/AW_C$, where M WCO_2 is the molecular weight of CO_2 and AW_C is the atomic weight of C.

production of 1 m^2 of finished ceramic tile product, with an average thickness of 9.5 mm, and the formulation indicated in Table 1. This LCA study is part of a comprehensive cradle-to-gate analysis for the production of 1 m^2 of porcelain stoneware, with a particular emphasis on the firing phase, identified as the most impactful stage. The focus of the study is on the "climate change" impact category, conducting a comparative study of two scenarios:

(A) Reference scenario: it outlines the firing phase of porcelain stoneware production, encompassing all inputs (materials, energy and resources) and outputs (fired tile, waste and emissions) associated with the process. The direct emissions of CO_2 considered in this scenario are solely from the stoichiometric combustion of natural gas employed

(B) LOI scenario: it also describes the firing phase of porcelain stoneware production, as detailed in the reference scenario. However, in addition to the CO_2 emissions from natural gas combustion, this scenario includes the CO_2 emissions from the thermal decomposition of inorganic carbonates and the combustion of organic matter. These additional emissions, calculated in this study, are incorporated into the Life Cycle Inventory (LCI) phase as direct emissions.

2.6.2. Life cycle inventory (LCI) and life cycle impact assessment (LCIA)

The data employed for the LCI phase were primary data, obtained directly from a ceramic company from the Sassuolo district, the centre of the Italian ceramic tile industry. The detailed inventories are presented in the supporting information Tables S6-S9. The processes were modelled by employing datasets from the Ecoinvent database (EID, version 3.10) (Weidema et al., 2025; Wernet et al., 2016), following an attributional approach (i.e., APOS system model) (Schaubroeck, 2023). The inventories were modelled in SimaPro 9.6.0.1 software (Pré Sustainability, S. 121, 3818 LE Amersfoort, Netherlands, 2025). The Life Cycle Impact Assessment (LCIA) was performed by using the EN 15804 + A2 method (adapted) (European Committee for Standardisation (CEN), 2019), the latter representing the most widely employed method for construction material processes and Environmental Product Declaration (EPD) in the construction sector (Durão et al., 2020; ISO 14025, 2006).

3. Results

3.1. Environmental impacts

The potential environmental impacts, calculated at the midpoint level (i.e., the compulsory stage in the impact assessment that focuses on specific environmental issues, before being aggregated into broader categories devoted to quantify the potential damage onto specific areas of protection, like human health and ecosystem), associated with the production of 24.5 kg (i.e., 1 m^2) of fired ceramic tiles via firing for the Reference scenario (A), are presented in Table 5, and the corresponding relative impacts are shown in Fig. 1. It is observed that the direct emissions of the process produce the main contribution to the "climate change", "eutrophication, marine", and "eutrophication, terrestrial" impact categories. Significant contributions to "acidification" and "photochemical ozone formation", "acidification" and some minor contribution to "human toxicity" (cancer and non-cancer), and "particulate matter" are also observed.

Particularly, for the "climate change" impact category, the impact equals 4.93 kg CO_2 eq, of which 87.2 % (i.e., 4.30 kg CO_2 eq) are attributed to the emission of CO_2 of fossil origins in air. 80.8 % (i.e., 3.47 kg CO_2 eq) of these emissions are associated with the direct emissions during the firing process and 13.9 % (0.59 kg CO_2 eq) are attributed to the lifecycle of natural gas (i.e., extraction and transportation). As for the latter, 22.8 % (i.e., 0.14 kg CO_2 eq) of the emissions caused by the use of natural gas are due to the EID dataset "Sweet gas, burned in gas turbine {GLO}| sweet gas, burned in gas turbine | APOS, U" (describing the combustion of sweet gas in turbine, necessary for the production of natural gas). Another 12.3 % (i.e., 0.60 kg CO_2 eq) of the impact category "climate change" is attributed to the emission of methane of fossil origin in air, which is mainly due (by 95.1 %) to the lifecycle of natural gas for the production of thermal energy, for 66.0 % associated with the EID dataset "Natural gas, vented {GLO}| natural gas venting from petroleum/natural gas production | APOS, U", describing the extraction of natural gas.

Normalization and weighting operations (the EF 3.1 normalization and weighting values, published in July 2022 (European Committee for Standardisation (CEN), 2019; European Platform on LCA | EPLCA, 2025), were used for the impact assessment method selected) led to the single score results illustrated in Fig. 2.

Direct emissions from the firing process contribute significantly to

Table 5
Environmental impacts, calculated at midpoint level (EN 15804 + A2), associated with the production of 1 m^2 (corresponding to 24.5 kg of fired ceramic tiles) in the reference scenario (A), which only considers the direct emissions of CO_2 from the combustion of natural gas while firing the ceramic tiles.

Impact category	Unit	Total
Climate change	kg CO_2 eq	4.93E+00
Ozone depletion	kg CFC11 eq	1.25E-07
Ionising radiation	kBq U-235 eq	1.71E-02
Photochemical ozone formation	kg NMVOC eq	1.23E-02
Particulate matter	disease inc.	1.97E-08
Human toxicity, non-cancer	CTUh	7.45E-09
Human toxicity, cancer	CTUh	6.98E-09
Acidification	mol H^+ eq	4.98E-03
Eutrophication, freshwater	kg P eq	7.13E-05
Eutrophication, marine	kg N eq	1.98E-03
Eutrophication, terrestrial	mol N eq	2.14E-02
Ecotoxicity, freshwater	CTUe	5.05E+00
Land use	Pt	1.28E+00
Water use	m^3 depriv.	1.40E-01
Resource use, fossils	MJ	7.50E+01
Resource use, minerals and metals	kg Sb eq	2.63E-06

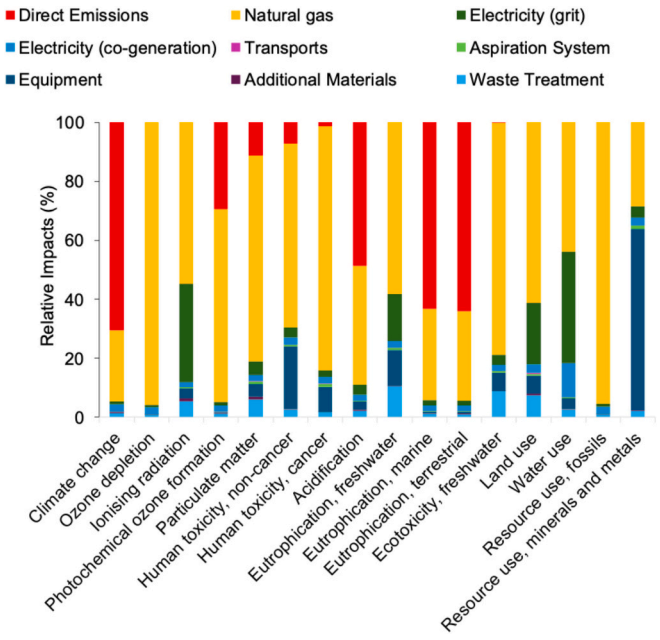

Fig. 1. The relative environmental impacts, calculated at midpoint level (EN 15804 + A2), associated with the production of 1 m^2 (corresponding to 24.5 kg of fired ceramic tiles) in the reference scenario (A), which only considers the direct emissions of CO_2 from the combustion of natural gas while firing the ceramic tiles.

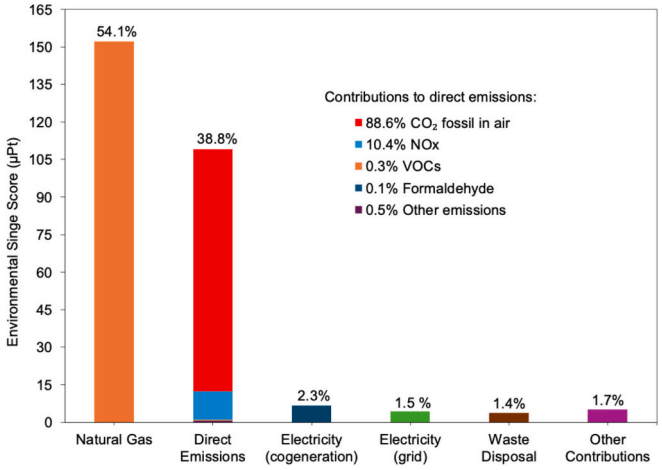

Fig. 2. The contributions to the environmental impacts of the firing process for Reference scenario (A) (EN 15804 + A2), namely "natural gas" (including production and pipeline transport), "direct emissions" (including CO_2 fossil in air; NOx; volatile organic compounds, VOCs; methane, fossil; other emissions), "electricity (co-generation)", "electricity (grid)", "waste disposal" and "other contributions" (equipment, additional materials such as hydrated lime, refractories).

the overall impact, accounting for 38.8 %. Of this, 88.6 % is due to the emissions of fossil-derived CO_2 into the air, while nitrogen oxides are responsible for 10.4 %. Additionally, the production and pipeline transport of natural gas account for 54.1 % of the total impact.

Other contributions are relatively less impactful. Co-generation electricity contributes by 2.3 %, the electricity from grid by 1.5 %, and the waste disposal by 1.4 %. Minor contributions, amounting to approximately 2.1 % of the environmental impact, arise from the construction of the equipment such as kiln, conveyor belt and aspiration system as well as from additional materials such as refractories and hydrated lime.

3.2. Comparative life cycle assessment: the role of physicochemical processes

The calculated CO_2 emissions resulting from the physicochemical processes that occur during firing were introduced in the LCI, considering a characterization factor (GWP) of 1, as it will be discussed in Section 4. The comparative LCA study between the reference scenario (A) and the LOI scenario (B) for firing of 1 m^2 of ceramic tiles, with an average thickness of 9.5 mm, corresponding to a mass of 24.5 kg, is illustrated in Fig. 3. The relative increase in climate change for the LOI scenario (B) is defined by Δ_{cc}, as delineated in Eq. (4). The analysis reveals that the climate change impact for the firing process under the LOI scenario is 8.4 % higher compared to the reference scenario. This increase in climate change impacts is attributed to CO_2 emissions generated during the combustion of organic matter and the decomposition of inorganic carbonate components in the ceramic body during firing. These findings highlight the importance of considering both fossil fuel-related emissions and those arising from physicochemical transformations of raw materials, for a comprehensive assessment of climate change impacts.

$$\Delta_{CC} = \frac{CO_2eq(B) - CO_2eq(A)}{CO_2eq(A)} \times 100 \quad (4)$$

3.3. Sensitivity analysis

To evaluate how Δ_{cc} (change in climate change impact score) varies with the origin of raw materials employed in the current ceramic mix, a sensitivity analysis was performed. The overall ceramic body

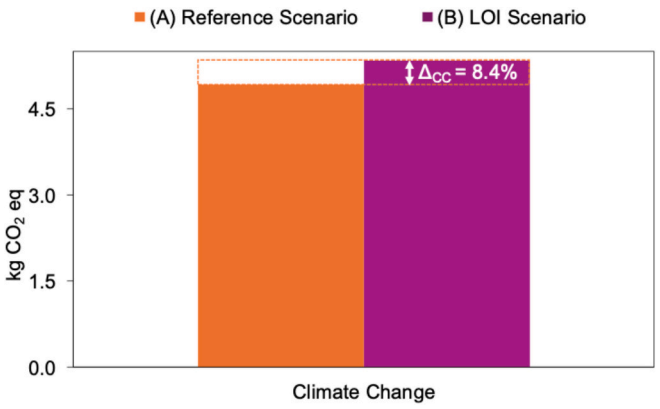

Fig. 3. The climate change impact category (EN 15804 + A2), for the production of 1 m^2 (corresponding to 24.5 kg of fired ceramic tiles) for (A) Reference scenario – the only direct emissions of CO_2 are associated with the combustion of natural gas; (B) LOI scenario – the calculated emissions of CO_2 associated with the thermal treatment of ceramic body are also included in the LCI as direct emissions.

composition, representative for porcelain stoneware—was kept constant: 41.0 % clays, 44.5 % feldspars, 12.6 % quartz-rich sands, alumina (1 %) and sodium silicate (<1 %)—while varying the types of clays and feldspars used (Cl1-Cl5 and Fd1-Fd5, as described in Table 1).

The analysis focused on the calculated content of OC and IC for individual raw materials (as described in Table 3 and Table S2). Specifically, combinations of five clays (Cl1–Cl5) and five feldspars (Fd1–Fd5) were evaluated, maintaining their respective proportions in the mix. The remaining components were held constant. Six scenarios were constructed by selecting clay–feldspar pairs with increasing total OC + IC content: minimum: Cl1 + Fd1, 25th quartile (Q1): Cl2 + Fd4, median: Cl3 + Fd3, 75th quartile (Q3): Cl4 + Fd4 and maximum: Cl5 + Fd5.

The LOI scenario (B), corresponding to the actual composition used in this study, was compared with the above defined scenarios. The results are depicted in Fig. 4 and Table S4 of the SI. The analysis shows that Δ_{cc} (calculated as indicated in Eq. (4)) varies significantly depending on the carbon content of raw materials. For the five types of clays and feldspars employed in this study, the minimum Δ_{cc} was 2.5 % and the maximum reached 26.5 %. The actual case study (8.4 %) lies below the median (11.81 %) indicating that the climate change impact score could be substantially higher if raw materials with elevated OC and IC content

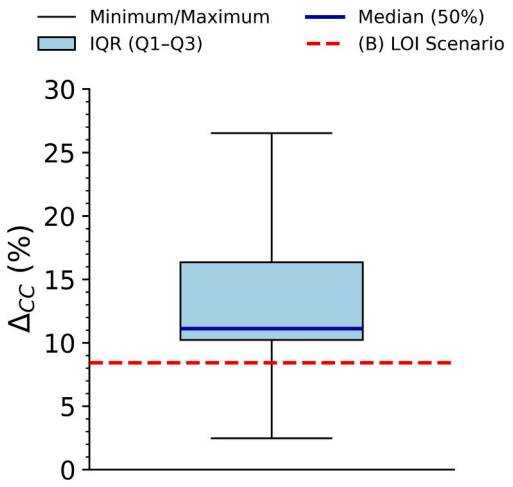

Fig. 4. Sensitivity analysis of Δ_{cc} for the firing stage of ceramic tile production, comparing the actual LOI scenario (B) with scenarios based on minimum, 25th percentile (Q1), median, 75th percentile (Q3), and maximum raw material total OC + IC content.

were used. This confirms the importance of including emissions from raw materials in the life cycle inventory (LCI), as conventional models that only account for fossil fuel combustion may underestimate the carbon footprint of ceramic tile production.

4. Discussion

4.1. Global warming potential (GWP) for the CO_2 emissions associated with the physicochemical process during firing stage

The results presented in Section 3.2 reveal and oversight in conventional environmental assessments of ceramic tile manufacturing. In the reference scenario (A), fossil-derived CO_2 emissions constitute 87.2 % of the climate change impacts during the firing phase. However, when emissions from physicochemical transformations—specifically the decomposition of inorganic carbonates and the combustion of organic matter—are included, the climate change impact increases by $\Delta_{cc} = 8.4$ % (see Fig. 3). This substantial rise demonstrates the limitations of current LCA practices that exclude these sources, leading to a systematic underestimation of the environmental burden.

The sensitivity analysis further reinforces that the significance of this discrepancy becomes even more pronounced when clay bodies rich in OM and carbonates, such as calcite and dolomite, are predominantly used. For instance, the difference in climate change impacts between the LOI scenario and reference scenario, Δ_{cc}, ranges from 2.5 % to 26.5 % for the raw materials selected in this study (see Section 3.3). Importantly, these materials introduce additional CO_2 emissions that originate from fundamentally different processes—organic combustion and mineral decomposition—each requiring distinct characterization factors. Accurately assessing these emissions demands a meticulous evaluation of the Global Warming Potential (GWP) assigned to them. Without such refinement, LCA models risk misrepresenting the true climate impact of ceramic production, particularly in formulations where these raw materials are prevalent.

The GWP is defined as "the ratio of the time-integrated radiative forcing from a pulse emission of 1 kg of a substance, relative to that of 1 kg of carbon dioxide, over a fixed horizon period" (Houghton et al., 1990). CO_2 is designated as the reference gas, with a GWP value of 1. Conventionally, as further discussed below, the emission of biogenic CO_2 are modelled assuming net-zero impacts, often without adequate justification, which can result in misleading conclusions (Cherubini et al., 2012).

The CO_2 emissions associated with the combustion of biomass are generally assumed to be climate change neutral. This convention is commonly adopted by most calculation methods employed in the LCA studies where there is an input of biomass, leading to an underestimation of the effect on climate change of the biomass combustion (Bright et al., 2012). There are currently two LCA methodologies (Hoxha et al., 2020; Bjarvin et al., 2025) that assess the emissions of biogenic CO_2:

1) The 0/0 approach assumes that the emissions of biogenic CO_2 are balanced by the absorption of CO_2 by biomass regrowth, resulting in a net zero impact on emissions (i.e., GWP $= 0$).
2) The 1/−1 approach tracks the flows of biogenic CO_2. GWP $= -1$ is assigned for the CO_2 uptake by the vegetation, whereas GWP $= 1$ is assigned for the release of CO_2 in the atmosphere. Since the emissions of biogenic CO_2 and the CO_2 uptake are part of a short cycle, the net impact remains neutral.

However, these approaches are not suitable for ceramic tile production, where clay extraction and firing represent irreversible processes that permanently remove organic carbon from the terrestrial pool. One of the most reliable ways of accounting for the environmental impacts of such transformations is to calculate the GWP of CO_2 emissions from OM combustion based on time-dependent carbon cycle modelling. The graphical representation of the OC flows of the studied system is delineated in Fig. 5.

To assess the impact associated with the emissions of CO_2 from the combustion of the OM within clay minerals, the methodology established by Cherubini et al. (Cherubini et al., 2012; Cherubini et al., 2011) was applied to the current system. The GWP for biogenic CO_2 is quantified as the ratio between the absolute GWP for biogenic CO_2 ($AGWP_{bioCO_2}$) and the absolute GWP for anthropogenic CO_2 ($AGWP_{CO_2}$) (Caldeira and Kasting, 1993). The absolute GWP (AGWP) is defined as the time integrated product of the radiative efficiency (a_{CO_2}) and the radiative decay function (B(t), for biogenic CO_2 and C(t), for anthropogenic CO_2) delineated in Eq. (5), where C_0 is the unit pulse (i.e., the amount of CO_2 released in one pulse), and TH is the time horizon introduced by IPCC (Eggelston et al., 2006) (20, 100, 500 years).

$$GWP_{bio} = \frac{AGWP_{bioCO_2}}{AGWP_{CO_2}} = \frac{C_0 \int_0^{TH} a_{CO_2} B(t)dt}{C_0 \int_0^{TH} a_{CO_2} C(t)dt} \quad (5)$$

According to the full impulse response function (FIRF) model (Tubiello and Oppenheimer, 1995), the emissions of CO_2 from OM combustion are removed from all three sinks – ocean, terrestrial biosphere, and vegetation regrowth (Cherubini et al., 2011). The atmospheric decay of the initial pulse of CO_2 in the atmosphere is expressed using Eq. (6), that is based on a Bern 2.5CC cycle model (Solomon, 2007) (a widely applied carbon cycle model), assuming a concentration of 378 ppm of atmospheric CO_2 and including the CO_2 uptake by on-site vegetation regrowth, ocean and terrestrial biosphere (Liu et al., 2017; Strassmann and Joos, 2018). In Eq. (6), the constant A_o is the fraction of CO_2 that remains in the atmosphere when the equilibrium is reached, A_1 –A_3 are the relative capacities of the three sinks to remove CO_2 from atmosphere, and τ_1–τ_3 are the corresponding relaxation times of the three sinks. The values of these constants are provided in Table S5 of the SI.

$$C(t) = A_o + \sum_{i=1}^{3} A_i e^{\left(-\frac{t}{\tau_i}\right)} \quad (6)$$

The atmospheric decay of a pulse of biogenic CO_2 over time is given by Eq. (7), where $g(t')$ is the probability density function that describes the vegetation regrowth in the analytical form shown in Eq. (8), where t' is the integration variable from the time since biomass removal occurred (i.e., the mineral extraction), t is the time dimension, r is the rotation period of the biomass (Cherubini et al., 2012; Cherubini et al., 2011).

$$B(t) = C(t) - \int_0^t g(t') \cdot C(t' - t)dt' \quad (7)$$

$$g(t') = \frac{1}{\sqrt{2\pi(r/2)^2}} exp\left(- \frac{(t' - r/2)^2}{2(r/4)^2} \right) \quad (8)$$

To accurately assess the GWP of CO_2 emissions from the combustion of OM in clay minerals, it is essential to consider the terrestrial carbon cycle. Here, we focus on two main factors: the OC turnover time in clay-rich soils and the potential for on-site vegetation regrowth following clay extraction.

1) OC turnover time. The mean turnover time for soil carbon has been estimated at 4178 ± 106 years (Li et al., 2023), with variations depending on climate zone, soil depth and mineral composition. In soils with high clay content, OM stabilization occurs through mechanisms like ligand exchange, cation bridging, electrostatic attraction, and hydrophobic interactions. The structure of phyllosilicates plays a critical role in inhibiting OM biodegradation (O'Loughlin et al., 2000; Nuruzade et al., 2023), involving complex mechanisms that render OM unavailable to microbial enzymes. These minerals also adsorb enzymes or inert molecules on their surface, alter microbial activity due to their interaction with

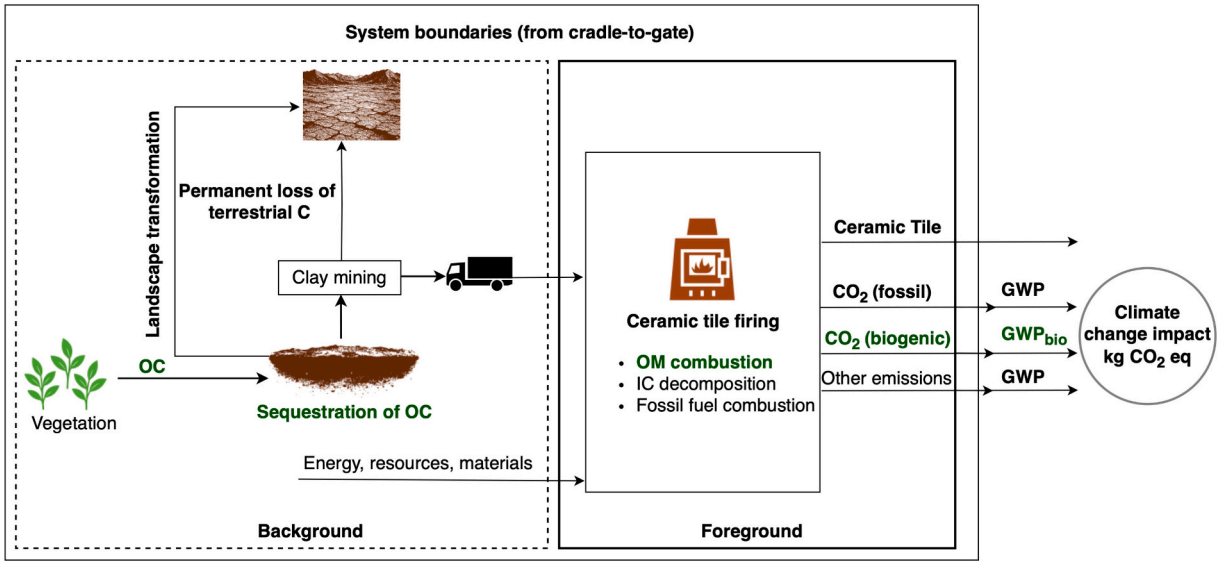

Fig. 5. Flowchart for the OC flows in the system under study, from cradle-to-gate boundaries. The foreground system refers to the firing of ceramic body, whereas the background system includes the extraction and transport of raw materials. C = carbon; OM = organic matter; OC = organic carbon; "other emissions" refers to additional GHG such as CH_4 and N_2O.

microorganisms, and buffer pH (Singh et al., 2018). As a result, OC associated with clay minerals may remain sequestered for extended periods, with turnover times reaching up to 10,000 years (Georgiou et al., 2022; Torn et al., 1997).

2) On-site vegetation regrowth. Open-pit clay mining causes a long-term landscape transformation (Turrión et al., 2021), involving the complete removal of topsoil and severely impacting groundwater and freshwater, sediments, and marine ecosystems. The loss of groundwater promotes clay dispersion and flocculation, increasing erosion risks for nearby topsoils. Consequently, this process leads to a substantial loss of soil organic carbon from the natural carbon cycle, reducing the terrestrial carbon pool at both the extraction site and surrounding areas due to erosion (Anju and Jaya, 2022). Regenerating vegetation in exhausted mining sites is highly challenging and requires intensive techniques for landscape recovery, including organic amendments and large amounts of fertilizers. In the absence of such interventions, the natural on-site regrowth of vegetation is very slow, therefore, the on-site CO_2 uptake by vegetation after its emission into the atmosphere is severely hampered and tends to zero.

Considering Eq. (8), in scenarios where vegetation is not regenerated after clay extraction, the biomass rotation period tends to infinity ($r \rightarrow \infty$). This represents a case of permanent terrestrial carbon loss, where the regrowth function approaches zero ($g(t') \rightarrow 0$) and the decay function for biogenic CO_2, B(t), becomes identical to that of anthropogenic CO_2, C (t) (i.e., $B(t) = C(t)$). As a result, GWP_{bio} is 1, which challenges the validity of 0/0 or $1/-1$ conventional approaches in LCA for this context.

The finding is strongly supported by the very long turnover times for OC in phyllosilicate-rich soils. In undisturbed conditions, OC would remain sequestrated for thousands of years. However, anthropogenic interventions such as clay mining and subsequent firing, disrupt the natural carbon cycle, permanently removing OC from the terrestrial carbon pool and releasing it as a single pulse of atmospheric CO_2.

Alkaline earth carbonates exhibit remarkable stability—even under acidic conditions (pH = 1), they release less than 1.5 % of their CO_2 content (Teir et al., 2006). Calcium carbonate, for example, requires high temperatures (900–950 °C) to decompose and release CO_2 (Erans et al., 2016), making it an effective long-term carbon store under natural conditions. However, during firing of ceramic bodies, this stored CO_2 from carbonates is released in the atmosphere in a single pulse, following the same atmospheric decay as the anthropogenic CO_2, thus being assigned a GWP of 1.

Ultimately, the findings of this study emphasize the importance of accurately accounting for all sources of CO_2 emissions in the firing phase of ceramic tile production. Additionally, these insights challenge the adequacy of conventional LCA assumptions regarding biogenic CO_2 neutrality. While fossil-derived CO_2 remains the dominant contributor to climate change in ceramic tile production, emissions from the decomposition of inorganic carbonates and the combustion of OM within clay minerals are far from negligible. Failing to account for the permanent loss of terrestrial carbon in these processes leads to a systematic underestimation of their climate impact. Assigning a GWP of 1 to these emissions is therefore not only justified, but essential for ensuring that LCA studies accurately reflect the true environmental burden of ceramic manufacturing, particularly in contexts involving irreversible land transformation and disrupted carbon cycles.

4.2. Model significance, applicability, limitations and development prospects

This section highlights the broader significance, accuracy, and practical applicability of the proposed approach for ceramic manufacturing, while also addressing its main limitations and directions for future research.

The typical composition of commercial porcelain stoneware tiles is 40–50 wt% kaolin clay, 35–45 wt% feldspar, and 10–15 wt% quartz (Martín-Márquez et al., 2008). The selected formulation for our case falls within this range, ensuring that the resulting properties are consistent with common porcelain stoneware. Significant deviations from this ceramic body mix composition would alter both product performance and waste generation, so the compositional window remains relatively narrow despite possible local variations in raw materials.

The raw materials used in this study—primarily of European origin—provide a robust basis for defining an average composition representative of European production of porcelain stoneware. However, the strength of this methodology lies in its flexibility: as long as the mineralogical and chemical composition is known, the model can be applied to other geographical contexts and alternative raw materials, including those not traditionally used in Europe (e.g., wollastonite in the USA).

The wide applicability of this methodology can be further enhanced by incorporating a broader set of representative formulas, especially for

illites and smectites. Its modular structure allows for the easy integration of new raw materials and extension to other ceramic products (e.g., bricks, roof tiles, refractories, sanitaryware), provided their raw materials are chemically and mineralogically characterized. Additionally, future research should focus on developing a dedicated protocol for low-firing ceramics, where incomplete dehydroxylation and partial structural water loss must be considered to ensure accurate emission estimates (Paige et al., 2017).

Under optimized conditions, this approach emerges as a promising tool for guiding raw material selection in ceramic tile manufacturing, with direct implications for emission reduction. Sensitivity analysis showed that the difference in climate change impact (Δ_{CC}) between the LOI scenario and the reference scenario varies widely with mineralogical composition, supporting long-term strategies to reduce the climate change impact of the firing stage and define emission thresholds.

While for the current case study, Δ_{CC} was found to be 8.4 %, it is important to emphasize that this value is specific to the composition of the ceramic body. The broader significance of this work primarily lies in the development of a transferable methodology, which can be applied to a variety of ceramic formulations and production contexts, potentially yielding different results depending on the specific characteristics of each case.

In practical terms, this methodology can support raw material selection during product formulation by identifying compositions with lower embedded CO_2 emissions. It can also be used to improve environmental reporting and carbon footprint declarations in compliance with ISO standards and EU regulations. Additionally, it offers a valuable tool for eco-design strategies, enabling manufacturers to simulate the impact of alternative formulations on overall emissions before implementation.

While this approach provides a robust and versatile framework for estimating CO_2 emissions from ceramic tile firing, some limitations should be considered. The current protocol is best suited for high-firing ceramics such as porcelain stoneware, where SWL is expected to be nearly complete. For lower-firing ceramics, incomplete dehydroxylation may occur, so the method may slightly overestimate SWL and underestimate residual organic matter. Additionally, the use of average stoichiometric formulas for the main mineral phases is a practical approximation, but in practice the composition can vary depending on the geological origin of the raw materials, and this may require additional sensitivity analyses.

To further improve accuracy, refinement of input data is essential—such as using site-specific information regarding the chemical and mineralogical composition of the raw materials employed. Moreover, accounting for batch-to-batch variability in composition of clays and other minerals would be beneficial to strengthen the accuracy of the climate change impacts prediction.

The further development prospects of this framework include its integration into established LCA databases, enabling more accurate and comprehensive carbon footprint calculations for a broad range of ceramic products. By coupling this methodology with an expanded mineralogical database, manufacturers will be able to assess the environmental impact of a wider range of raw materials and formulations, supporting more informed choices in material selection and transparent environmental reporting in line with regulatory and market requirements. Importantly, our findings indicate that the CO_2 emissions from both carbonates and organic matter in raw materials should be calculated and accounted for when assessing the carbon footprint of ceramic tiles, and these emissions should be included in Environmental Product Declarations (EPDs). Extending this analysis to other ceramic products—such as bricks, refractories, and sanitaryware—will further improve the accuracy of carbon emission assessments across the ceramic industry and support more sustainable manufacturing practices.

5. Conclusions

A more rigorous evaluation of the environmental impacts associated with the industrial production of ceramic tiles was proposed and conducted by employing the life cycle assessment (LCA) methodology.

This study is the first to include the emissions associated with the physicochemical processes occurring during the firing stage of the ceramic body.

To facilitate this, a new protocol was developed to estimate the structural water loss (SWL) which heavily affects the calculation of organic matter (OM) content when using the conventional "loss on ignition" (LOI) method. This approach is grounded in the chemical and mineralogical composition of the ceramic body, including the structural differences among various types of clay minerals and their distinct thermal behaviour. Emissions from the thermal decomposition of carbonates were also considered.

Without accounting for emissions from physicochemical processes, the climate change impacts associated with producing 1 m^2 (24.5 kg) of fired ceramic tiles was calculated at 4.93 kg of CO_2 equivalent, with 87.2 % of the impact attributed to fossil CO_2 emissions from natural gas and 12.3 % of the overall contribution to climate change is linked to methane emissions from fossil sources, mainly due to leakage during pipeline transportation.

A comparative LCA showed that including the materials-related CO_2 emissions led to an 8.4 % increase in climate change impacts compared to the reference scenario. The sensitivity analysis showed that this difference can vary from 2.5 % to 26.5 %, depending on carbon content and geographic origin of raw materials.

While the specific emission values obtained in this study are limited to the ceramic body mix analysed, the proposed methodology for estimating the OM content—based on structural water loss and mineralogical composition—can be broadly applied to other ceramic formulations, offering a more accurate assessment of raw material-related CO_2 emissions in ceramic tile production.

The global warming potential (GWP) of CO_2 emissions associated with the combustion of organic matter present within minerals was assessed using a combined biomass growth model with Bern 2.5CC model was employed, following the methodology developed by Cherubini et al. (2011). It was concluded that the GWP of biogenic CO_2 from OM in minerals should be treated as equivalent to fossil-derived CO_2 (GWP $= 1$). Notably, this study is the first to propose assigning a GWP of 1 to CO_2 emissions from OM embedded in mineral matrices. This represents a significant advancement in carbon accounting for the ceramic industry, challenging the conventional climate-neutrality assumption often applied to biogenic CO_2 and highlights the need to treat these emissions as equivalent to fossil-derived CO_2 in LCA studies.

These findings highlight the critical need to incorporate emissions from physicochemical transformations into life cycle inventories across the ceramic sector. By addressing previously overlooked sources of CO_2, this study contributes to a more robust evaluation of carbon footprints. The proposed methodology not only refines emissions quantification but also provides a transferable framework for evaluating climate change impacts in other ceramic applications, supporting the development of targeted sustainability strategies and industry-specific guidelines.

CRediT authorship contribution statement

Andrei Ungureanu: Conceptualization, Data curation, Formal analysis, Investigation, Methodology, Validation, Visualization, Software, Writing – original draft, Writing – review & editing. **Antonella Sola:** Investigation, Methodology, Writing – original draft, Writing – review & editing. **Paolo Neri:** Formal analysis, Investigation, Software, Writing – review & editing. **Roberto Rosa:** Investigation, Supervision, Writing – original draft, Writing – review & editing. **Alessandro Gualtieri:** Methodology, Writing – original draft, Writing – review & editing. **Anna Maria Ferrari:** Supervision, Funding acquisition, Resources,

Writing – review & editing.

Declaration of competing interest

The authors declare no competing interests.

Acknowledgements

This work was supported by the Programma Operativo Nazionale Ricerca e Innovazione 2014-2020 (CCI 2014IT16M2OP005), under CUP E85F21003350001, for which the authors are sincerely grateful.

Appendix A. Supplementary data

Supplementary data to this article can be found online at https://doi.org/10.1016/j.eiar.2025.108235.

Data availability

The data supporting this article have been included within the article and as part of the Supplementary Information.

References

Akisanmi, P., 2022. Classification of clay minerals. In: René, M. (Ed.), Mineralogy. IntechOpen. https://doi.org/10.5772/intechopen.103841.
Almeida, M.I., Dias, A.C., Demertzi, M., Arroja, L., 2016. Environmental profile of ceramic tiles and their potential for improvement. J. Clean. Prod. 131, 583–593. https://doi.org/10.1016/j.jclepro.2016.04.131.
Andji, J.Y.Y., Toure, A.A., Kra, G., Jumas, J.C., Yvon, J., Blanchart, P., 2009. Iron role on mechanical properties of ceramics with clays from Ivory Coast. Ceram. Int. 35 (2), 571–577. https://doi.org/10.1016/j.ceramint.2008.01.007.
Anju, P.S., Jaya, D.S., 2022. Impacts of clay mining activities on aquatic ecosystems: a critical review. IJEAT 11 (4), 128–134. https://doi.org/10.35940/ijeat.D3495.0411422.
Arabmofrad, S., Bagheri, M., Rajabi, H., Jafari, S.M., 2020. Nanoadsorbents and Nanoporous materials for the food industry. In: Handbook of Food Nanotechnology. Elsevier, pp. 107–159. https://doi.org/10.1016/B978-0-12-815866-1.00004-2.
Ball, D.F., 1964. Loss-on-ignition as an estimate of organic matter and organic carbon in npn-calcareous soils. J. Soil Sci. 15 (1), 84–92. https://doi.org/10.1111/j.1365-2389.1964.tb00247.x.
Bjarvin, C., Pierobon, F., Ganguly, I., 2025. Global warming potential estimates of mass timber constructions beyond the first life: a dynamic radiative forcing modeling approach. Environ. Impact Assess. Rev. 115, 107968. https://doi.org/10.1016/j.eiar.2025.107968.
Brigatti, M.F., Galán, E., Theng, B.K.G., 2013. Structure and mineralogy of clay minerals. In: Developments in Clay Science, vol. 5. Elsevier, pp. 21–81.
Bright, R.M., Cherubini, F., Strømman, A.H., 2012. Climate impacts of bioenergy: inclusion of carbon cycle and albedo dynamics in life cycle impact assessment. Environ. Impact Assess. Rev. 37, 2–11. https://doi.org/10.1016/j.eiar.2012.01.002.
Brindley, G.W., Gillery, F.H., 2025. X-ray identification of chlorite species. Am. Mineral. 41 (3–4), 169–186.
Caldeira, K., Kasting, J.F., 1993. Insensitivity of global warming potentials to carbon dioxide emission scenarios. Nature 366 (6452), 251–253. https://doi.org/10.1038/366251a0.
Celik, H., 2010. Technological characterization and industrial application of two Turkish clays for the ceramic industry. Appl. Clay Sci. 50 (2), 245–254. https://doi.org/10.1016/j.clay.2010.08.005.
Cheng, Y., Xing, J., Bu, C., Zhang, J., Piao, G., Huang, Y., Xie, H., Wang, X., 2019. Dehydroxylation and structural distortion of kaolinite as a high-temperature sorbent in the furnace. Minerals 9 (10), 587. https://doi.org/10.3390/min9100587.
Cherubini, F., Peters, G.P., Berntsen, T., Strømman, A.H., Hertwich, E., 2011. CO2 emissions from biomass combustion for bioenergy: atmospheric decay and contribution to global warming. GCB Bioenergy 3 (5), 413–426. https://doi.org/10.1111/j.1757-1707.2011.01102.x.
Cherubini, F., Bright, R.M., Strømman, A.H., 2012. Site-specific global warming potentials of biogenic CO $_2$ for bioenergy: contributions from carbon fluxes and albedo dynamics. Environ. Res. Lett. 7 (4), 045902. https://doi.org/10.1088/1748-9326/7/4/045902.
Cuadros, J., Huertas, F., Delgado, A., Linares, J., 1994. Determination of hydration (H $_2$ O $^-$) and structural (H $_2$ O $^+$) water for chemical analysis of Smectites. Application to Los Trancos Smectites, Spain. Clay Miner. 29 (2), 297–300. https://doi.org/10.1180/claymin.1994.029.2.16.
Das, S.K., Dana, K., 2003. Differences in densification behaviour of K- and Na-feldspar-containing porcelain bodies. Thermochim. Acta 406 (1–2), 199–206. https://doi.org/10.1016/S0040-6031(03)00257-0.
Derkowski, A., Kuligiewicz, A., 2022. Thermal analysis and thermal reactions of Smectites: a review of methodology, mechanisms, and kinetics. Clay Clay Miner. 70 (6), 946–972. https://doi.org/10.1007/s42860-023-00222-y.
Di Primio, S., 2018. Minerali Industriali - Impasti per grès porcellanato smaltato idonei per la produzione in linea continua. In: Impasti per grès porcellanato smaltato idonei per la produzione in linea continua. Minerali Industriali.
Djemli, A., Ghebouli, M.A., Bouferrache, K., Slimani, Y., Habila, M.A., M, F., Chihi, T., Ghebouli, B., Sillanpää, M., 2023. Effect of temperature and glass content on crystalline phases in porcelain sintered with recovered automotive glass. Heliyon 9 (12), e22554. https://doi.org/10.1016/j.heliyon.2023.e22554.
Dondi, Michele, Fabbri, Bruno, 1993. Clays for the Heavy-Clay Industry in Tuscany and Umbria (Central Italy). In: Clays: Controlling the Environment. CSIRO Publishing, Adelaide, Australia, pp. 122–128.
Dondi, Michele, Ercolani, G., Fabbri, B., Guarini, G., Marsigli, M., Mingazzini, C., 1999. Major deposits of brick clays in Italy. Part 1: geology and composition. Tile Brick Int. 15, 230–237.
Drits, V.A., Besson, G., Muller, F., 1995. An improved model for structural transformations of heat-treated aluminous Dioctahedral 2:1 layer silicates. Clay Clay Miner. 43 (6), 718–731. https://doi.org/10.1346/CCMN.1995.0430608.
Durão, V., Silvestre, J.D., Mateus, R., De Brito, J., 2020. Assessment and communication of the environmental performance of construction products in Europe: comparison between PEF and EN 15804 compliant EPD schemes. Resour. Conserv. Recycl. 156, 104703. https://doi.org/10.1016/j.resconrec.2020.104703.
Eggelston, Simon, Buendia, Leandro, Miwa, Kyoko, Ngara, Todd, Tanabe, Kiyoto, 2006. 2006 IPCC Guidelines for National Greenhouse gas Inventories. Institute for Global Environmental Strategies (IGES) for the IPCC, Japan.
Erans, M., Manovic, V., Anthony, E.J., 2016. Calcium looping sorbents for CO2 capture. Appl. Energy 180, 722–742. https://doi.org/10.1016/j.apenergy.2016.07.074.
European Committee for Standardisation (CEN), 2019. EN 15804 + A2: 2019—Sustainability of Construction Works—Environmental Product Declarations—Core Rules for the Product Category of Construction Prod; Brussels.
European Platform on LCA | EPLCA, 2025. https://eplca.jrc.ec.europa.eu/EFtransition.html (accessed 2024-09-18).
Ferrer, S., Mezquita, A., Gomez-Tena, M.P., Machi, C., Monfort, E., 2015. Estimation of the heat of reaction in traditional ceramic compositions. Appl. Clay Sci. 108, 28–39. https://doi.org/10.1016/j.clay.2015.02.019.
Furszyfer Del Rio, D.D., Sovacool, B.K., Foley, A.M., Griffiths, S., Bazilian, M., Kim, J., Rooney, D., 2022. Decarbonizing the ceramics industry: a systematic and critical review of policy options, developments and sociotechnical systems. Renew. Sust. Energ. Rev. 157, 112081. https://doi.org/10.1016/j.rser.2022.112081.
Galos, K., 2011. Composition and ceramic properties of Ball clays for porcelain stoneware tiles manufacture in Poland. Appl. Clay Sci. 51 (1–2), 74–85. https://doi.org/10.1016/j.clay.2010.11.004.
Garg, N., Skibsted, J., 2014. Thermal activation of a pure montmorillonite clay and its reactivity in cementitious systems. J. Phys. Chem. C 118 (21), 11464–11477. https://doi.org/10.1021/jp502529d.
Gasparini, E., Tarantino, S.C., Ghigna, P., Riccardi, M.P., Cedillo-González, E.I., Siligardi, C., Zema, M., 2013. Thermal dehydroxylation of kaolinite under isothermal conditions. Appl. Clay Sci. 80–81, 417–425. https://doi.org/10.1016/j.clay.2013.07.017.
Georgiou, K., Jackson, R.B., Vindušková, O., Abramoff, R.Z., Ahlström, A., Feng, W., Harden, J.W., Pellegrini, A.F.A., Polley, H.W., Soong, J.L., Riley, W.J., Torn, M.S., 2022. Global stocks and capacity of mineral-associated soil organic carbon. Nat. Commun. 13 (1), 3797. https://doi.org/10.1038/s41467-022-31540-9.
Gridi-Bennadji, F., Beneu, B., Laval, J.P., Blanchart, P., 2008. Structural transformations of muscovite at high temperature by X-ray and Neutron diffraction. Appl. Clay Sci. 38 (3–4), 259–267. https://doi.org/10.1016/j.clay.2007.03.003.
Gualtieri, A.F., 2007. Thermal behavior of the raw materials forming porcelain stoneware mixtures by combined optical and *in situ* X-ray dilatometry. J. Am. Ceram. Soc. 90 (4), 1222–1231. https://doi.org/10.1111/j.1551-2916.2007.01614.x.
Gualtieri, A.F., Ferrari, S., 2006. Kinetics of Illite Dehydroxylation. Phys. Chem. Miner. 33 (7), 490–501. https://doi.org/10.1007/s00269-006-0092-z.
Gualtieri, A.F., Gandolfi, N.B., Pollastri, S., Rinaldi, R., Sala, O., Martinelli, G., Bacci, T., Paoli, F., Viani, A., Vigliaturo, R., 2018. Assessment of the potential hazard represented by natural raw materials containing mineral fibres—the case of the feldspar from Orani, Sardinia (Italy). J. Hazard. Mater. 350, 76–87. https://doi.org/10.1016/j.jhazmat.2018.02.012.
Heaton, L., Fullen, M.A., Bhattacharyya, R., 2016. Critical analysis of the van Bemmelen conversion factor used to convert soil organic matter data to soil organic carbon data: comparative analyses in a UK loamy sand soil. EspacoAberto 6 (1), 35–44. https://doi.org/10.36403/espacoaberto.2016.5244.
Heiri, O., Lotter, A.F., Lemcke, G., 2001. Loss on ignition as a method for estimating organic and carbonate content in sediments: reproducibility and comparability of results. J. Paleolimnol. 25, 101–110. https://doi.org/10.1023/A:1008119611481.
Hellweg, S., Milà, I., Canals, L., 2014. Emerging approaches, challenges and opportunities in life cycle assessment. Science 344 (6188), 1109–1113. https://doi.org/10.1126/science.1248361.
Hoogsteen, M.J.J., Lantinga, E.A., Bakker, E.J., Groot, J.C.J., Tittonell, P.A., 2015. Estimating soil organic carbon through loss on ignition: effects of ignition conditions and structural water loss. Eur. J. Soil Sci. 66 (2), 320–328. https://doi.org/10.1111/ejss.12224.
Houghton, J.T., Jenkins, G.J., Ephraums, J.J., 1990. IPCC, 1990: Scientific Assessment of Climate Change – Report of Working Group I. Cambridge University Press, Cambridge, United Kingdom, and New York, NY, USA.
Hoxha, E., Passer, A., Saade, M.R.M., Trigaux, D., Shuttleworth, A., Pittau, F., Allacker, K., Habert, G., 2020. Biogenic carbon in buildings: a critical overview of LCA methods. Buildings Cities 1 (1), 504–524. https://doi.org/10.5334/bc.46.

ISO 14025, 2006. Environmental Labels and Declarations – Type III Environmental Declarations – Principles and Procedures. International Organization for Standardization, Genève, Switzerland.
ISO 14040, 2006. Environmental Management Life Cycle Assessment Principles and Framework. International Organisation for Standardisation (ISO), Genève, Switzerland.
ISO 14044, 2006. Environmental Management—Life Cycle Assessment—Requirements and Guidelines. International Organisation for Standardisation (ISO), Genève, Switzerland.
Jensen, J.L., Christensen, B.T., Schjønning, P., Watts, C.W., Munkholm, L.J., 2018. Converting loss-on-ignition to organic carbon content in arable topsoil: pitfalls and proposed procedure. Eur. J. Soil Sci. 69 (4), 604–612. https://doi.org/10.1111/ejss.12558.
Karnland, O., 2025. Chemical and Mineralogical Characterization of the Bentonite Buffer for the Acceptance Control Procedure in a KBS-3 Repository. Technical Report TR-10-60.
Kates, R.W., Mayfield, M.W., Torrie, R.D., Witcher, B., 1998. Methods for estimating greenhouse gases from local places. Local Environ. 3 (3), 279–297. https://doi.org/10.1080/13549839808725566.
Keeling, C.D., 1973. Industrial production of carbon dioxide from fossil fuels and limestone. Tellus 25 (2), 174–198. https://doi.org/10.1111/j.2153-3490.1973.tb01604.x.
Li, J., Ding, J., Yang, S., Zhao, L., Li, J., Huo, H., Wang, M., Tan, J., Cao, Y., Ren, S., Liu, Y., Wang, T., 2023. Depth-dependent driver of global soil carbon turnover times. Soil Biol. Biochem. 185, 109149. https://doi.org/10.1016/j.soilbio.2023.109149.
Liu, W., Zhang, Z., Xie, X., Yu, Z., Von Gadow, K., Xu, J., Zhao, S., Yang, Y., 2017. Analysis of the global warming potential of biogenic CO2 emission in life cycle assessments. Sci. Rep. 7 (1), 39857. https://doi.org/10.1038/srep39857.
Martín-Márquez, J., Rincón, J.Ma., Romero, M., 2008. Effect of firing temperature on sintering of porcelain stoneware tiles. Ceram. Int. 34 (8), 1867–1873. https://doi.org/10.1016/j.ceramint.2007.06.006.
Minerali Industriali S.r.l, 2016. Technical Data Sheet - Sport & Leisure Products Line - Feldspathic Sand (4/30N).
Nuruzade, O., Abdullayev, E., Erastova, V., 2023. Organic–mineral interactions under natural conditions: a computational study of flavone adsorption on smectite clay. J. Phys. Chem. C 127 (27), 13167–13177. https://doi.org/10.1021/acs.jpcc.3c00174.
Odent, B.E., 1994. Mémento roches et minéraux industriels feldspaths et roches à feldspathoïdes. R 38221;. BRGM.
Ogloza, A.A., Malhotra, V.M., 1989. Dehydroxylation induced structural transformations in montmorillonite: an isothermal FTIR study. Phys. Chem. Miner. 16 (4). https://doi.org/10.1007/BF00199559.
O'Loughlin, E.J., Traina, S.J., Sims, G.K., 2000. Effects of sorption on the biodegradation of 2-methylpyridine in aqueous suspensions of reference clay minerals. Environ. Toxic Chem. 19 (9), 2168–2174. https://doi.org/10.1002/etc.5620190904.
Paige, J., Michelaki, K., Campisano, C., Barton, M., Heimsath, A., 2017. Are the intensities and durations of small-scale pottery firings sufficient to completely dehydroxylate clays? Testing a key assumption underlying ceramic rehydroxylation dating. J. Archaeol. Sci. 79, 44–52. https://doi.org/10.1016/j.jas.2017.01.009.
Palomba, M., Padalino, G., Baldracchi, A., 2010. An unusual occurrence of an exploitable K-feldspar deposit hosted in the Ordovician Porphyroids (southern Sardinia). Ore Geol. Rev. 37 (3–4), 202–213. https://doi.org/10.1016/j.oregeorev.2010.03.003.
Pré Sustainability, S. 121, 3818 LE Amersfoort, Netherlands, 2025. SimaPro | LCA Software for Informed Changemakers. https://simapro.com/ (accessed 2024-09-26).
Ramamoorthi, V., Meena, S., 2018. Quantification of soil organic carbon - comparison of wet oxidation and dry combustion methods. Int. J. Curr. Microbiol. App. Sci. 7 (10), 146–154. https://doi.org/10.20546/ijcmas.2018.710.016.
Rat, E., Martínez-Martínez, S., Sánchez-Garrido, J.A., Pérez-Villarejo, L., Garzón, E., Sánchez-Soto, P.J., 2023. Characterization, thermal and ceramic properties of clays from Alhabia (Almería, Spain). Ceram. Int. 49 (9), 14814–14825. https://doi.org/10.1016/j.ceramint.2022.05.328.
Rauf, A., Shakir, S., Ncube, A., Abd-ur-Rehman, H.M., Janjua, A.K., Khanum, S., Khoja, A.H., 2022. Prospects towards sustainability: a comparative study to evaluate the environmental performance of brick making kilns in Pakistan. Environ. Impact Assess. Rev. 94, 106746. https://doi.org/10.1016/j.eiar.2022.106746.
Schaubroeck, T., 2023. Relevance of attributional and consequential life cycle assessment for society and decision support. Front. Sustain. 4, 1063583. https://doi.org/10.3389/frsus.2023.1063583.
Singh, M., Sarkar, B., Sarkar, S., Churchman, J., Bolan, N., Mandal, S., Menon, M., Purakayastha, T.J., Beerling, D.J., 2018. Stabilization of soil organic carbon as influenced by clay mineralogy. In: Advances in Agronomy, 148. Elsevier, pp. 33–84. https://doi.org/10.1016/bs.agron.2017.11.001.
Soil and Environmental Chemistry, 2017. Elsevier. https://doi.org/10.1016/C2015-0-01022-X.
Solomon, S., 2007. In: Intergovernmental Panel on Climate Change, Intergovernmental Panel on Climate Change (Eds.), Climate Change 2007: The Physical Science Basis: Contribution of Working Group I to the Fourth Assessment Report of the Intergovernmental Panel on Climate Change. Cambridge University Press, Cambridge; New York.
Steudel, A., Kleeberg, R., Koch, C.B., Friedrich, F., Emmerich, K., 2016. Thermal behavior of chlorites of the Clinochlore-Chamosite solid solution series: oxidation of structural Iron, hydrogen release and dehydroxylation. Appl. Clay Sci. 132–133, 626–634. https://doi.org/10.1016/j.clay.2016.08.013.
Stevenson, C.M., Gurnick, M., 2016. Structural collapse in kaolinite, montmorillonite and Illite clay and its role in the ceramic rehydroxylation dating of low-fired earthenware. J. Archaeol. Sci. 69, 54–63. https://doi.org/10.1016/j.jas.2016.03.004.
Strassmann, K.M., Joos, F., 2018. The Bern Simple Climate Model (BernSCM) v1.0: an extensible and fully documented open-source re-implementation of the bern reduced-form model for global carbon cycle–climate simulations. Geosci. Model Dev. 11 (5), 1887–1908. https://doi.org/10.5194/gmd-11-1887-2018.
Sun, H., Nelson, M., Chen, F., Husch, J., 2009. Soil mineral structural water loss during loss on ignition analyses. Can. J. Soil Sci. 89 (5), 603–610. https://doi.org/10.4141/CJSS09007.
Tate, R.L., 2005. Encyclopedia of soils in the environment: volume 1-4. Soil Sci. 170 (8), 669. https://doi.org/10.1097/01.ss.0000178203.51170.63.
Taylor, H.F.W., 1962. Homogeneous and inhomogeneous mechanisms in the dehydroxylation of minerals. Clay Miner. 5 (28), 45–55. https://doi.org/10.1180/claymin.1962.005.28.01.
Teir, S., Eloneva, S., Fogelholm, C.-J., Zevenhoven, R., 2006. Stability of calcium carbonate and magnesium carbonate in rainwater and nitric acid solutions. Energy Convers. Manag. 47 (18–19), 3059–3068. https://doi.org/10.1016/j.enconman.2006.03.021.
Torn, M.S., Trumbore, S.E., Chadwick, O.A., Vitousek, P.M., Hendricks, D.M., 1997. Mineral control of soil organic carbon storage and turnover. Nature 389 (6647), 170–173. https://doi.org/10.1038/38260.
Tubiello, F.N., Oppenheimer, M., 1995. Impulse-response functions and anthropogenic CO $_2$. Geophys. Res. Lett. 22 (4), 413–416. https://doi.org/10.1029/94GL03276.
Turrión, D., Morcillo, L., Alloza, J.A., Vilagrosa, A., 2021. Innovative techniques for landscape recovery after clay mining under mediterranean conditions. Sustainability 13 (6), 3439. https://doi.org/10.3390/su13063439.
Viani, A., Gualtieri, A.F., Artioli, G., 2025. The Nature of Disorder in Montmorillonite by Simulation of X-Ray Powder Patterns.
Vieira, A.W., Rosso, L.S., Demarch, A., Pasini, D., Ruzza, S.P., Arcaro, S., Ribeiro, M.J., Angioletto, E., 2023. Life cycle assessment in the ceramic tile industry: a review. J. Mater. Res. Technol. 23, 3904–3915. https://doi.org/10.1016/j.jmrt.2023.02.023.
Wang, G., Wang, H., Zhang, N., 2017. In situ high temperature X-ray diffraction study of Illite. Appl. Clay Sci. 146, 254–263. https://doi.org/10.1016/j.clay.2017.06.006.
Wang, B., Shan, T., Wang, J., Huang, F., Liu, W., Tu, W., Li, S., Chen, Q., 2023. Sources, distribution and decomposition of soil organic matter based on an effective biomarker in the pastoral areas of Zoige plateau, China. Chemosphere 312, 137295. https://doi.org/10.1016/j.chemosphere.2022.137295.
Weidema, B., Hischier, R., Mutel, C., Bauer, C., Nemecek, T., Reinhard, J., Vadenbo, C., Wernet, G., 2025. The Ecoinvent Database: Overview and Methodology, Data Quality Guideline for the Ecoinvent Database Version 3. https://ecoinvent.org/ (accessed 2024-09-25).
Wernet, G., Bauer, C., Steubing, B., Reinhard, J., Moreno-Ruiz, E., Weidema, B., 2016. The ecoinvent database version 3 (part I): overview and methodology. Int. J. Life Cycle Assess. 21 (9), 1218–1230. https://doi.org/10.1007/s11367-016-1087-8.
Zaidan, S.A., Abdull-Razzak, S.S., 2018. Effect of bentonite addition on some properties of porcelain. jcoeng 25 (1), 84–99. https://doi.org/10.31026/j.eng.2019.01.07.
Zanelli, C., Iglesias, C., Domínguez, E., Gardini, D., Raimondo, M., Guarini, G., Dondi, M., 2015. Mineralogical composition and particle size distribution as a key to understand the technological properties of Ukrainian Ball clays. Appl. Clay Sci. 108, 102–110. https://doi.org/10.1016/j.clay.2015.02.005.
Zhan, W., Guggenheim, S., 1995. The dehydroxylation of chlorite and the formation of topotactic product phases. Clay Clay Miner. 43 (5), 622–629. https://doi.org/10.1346/CCMN.1995.0430512.
Zhang, W., Liang, W., Zhang, Z., Hao, T., 2021. Aerobic granular sludge (AGS) scouring to mitigate membrane fouling: performance, hydrodynamic mechanism and contribution quantification model. Water Res. 188, 116518. https://doi.org/10.1016/j.watres.2020.116518.